R–1386

# ULTIMATE INTRINSIC–COERCIVITY SAMARIUM–COBALT MAGNET

## AN EARTH–BASED FEASIBILITY STUDY FOR SPACE–SHUTTLE MISSIONS

by

D. Das, K. Kumar
The Charles Stark Draper Laboratory, Inc.

R.T. Frost and C.W. Chang
Space Sciences Division, General Electric Company

May 1980

For the Period
October 1, 1979 to April 30, 1980

Prepared for National Aeronautics
and Space Administration,
Under Contract NAS8–33607



**The Charles Stark Draper Laboratory, Inc.**
Cambridge, Massachusetts 02139

TECHNICAL REPORT STANDARD TITLE PAGE

| 1. Report No. | 2. Government Accession No. | 3. Recipient's Catalog No. |
|---|---|---|
| 4. Title and Subtitle<br>ULTIMATE INTRINSIC-COERCIVITY SAMARIUM-COBALT MAGNET<br>AN EARTH-BASED FEASIBILITY STUDY FOR SPACE-SHUTTLE MISSIONS | | 5. Report Date<br>May 1980<br>6. Performing Organization Code |
| 7. Author(s)<br>D. Das, K. Kumar, R.T. Frost, and C.W. Chang | | 8. Performing Organization Report No.<br>R-1386 |
| 9. Performing Organization Name and Address<br>The Charles Stark Draper Laboratory, Inc.<br>555 Technology Square<br>Cambridge, Massachusetts 02139 | | 10. Work Unit No.<br>11. Contract or Grant No.<br>NAS8-33607 |
| 12. Sponsoring Agency Name and Address<br>National Aeronautics and Space Administration<br>George C. Marshall Space Flight Center<br>Marshall Space Flight Center, Alabama 35812 | | 13. Type of Report and Period Covered<br>Technical Report<br>1 October 1979 to<br>30 April 1980<br>14. Sponsoring Agency Code |

15. Supplementary Notes

16. Abstract

An important milestone of the program has now been achieved with the successful development of techniques for containerless melting and solidification of the samarium-cobalt alloy without excessive oxidation. Development of techniques for the containerless reaction of elemental samarium and cobalt to form the alloy will be initiated as soon as incremental funding becomes available. The rationale for extending these experiments in a weightless environment is also discussed.

The effect of oxygen content from 0.15 to 0.63 weight percent and grain size in the range of 2 to 10 micrometers has been examined on arc-plasma-sprayed $SmCo_5$ magnets. Contrary to expectations, the larger grain sizes tended to improve the coercivities. This was attributed to an increase in homogeneity resulting from higher temperature treatments used to produce larger grain size. No significant differences in coercivity were observed on the basis of oxygen content in the range examined. It is expected that more meaningful data on the relationship between oxygen content and coercivity will be seen when the oxygen content can be lowered to less than 0.1 weight percent as discussed in the report.

| 17. Key Words Suggested by Author | 18. Distribution Statement |
|---|---|
| Magnet<br>Samarium-Cobalt<br>Coercivity<br>Levitation Melting<br>Oxygen-Free Comminution<br>Arc-Plasma Spraying | |

| 19. Security Classif. (of this report) | 20. Security Classif. (of this page) | 21. No. of Pages | 22. Price |
|---|---|---|---|
| UNCLASSIFIED | UNCLASSIFIED | | |

R-1386

# ULTIMATE INTRINSIC-COERCIVITY SAMARIUM-COBALT MAGNET

## AN EARTH-BASED FEASIBILITY STUDY FOR SPACE-SHUTTLE MISSIONS

May 1980

For the Period
October 1, 1979 to April 30, 1980

by

Dilip K. Das*
Kaplesh Kumar*

The Charles Stark Draper Laboratory, Inc.

Robert T. Frost
C. W. Chang

Space Sciences Division
General Electric Company

Prepared for National Aeronautics
and Space Administration,
Under Contract NAS8-33607

*Some of the work reported in this report was performed at the Francis Bitter National Magnet Laboratory by the authors as Visiting Scientists.

**Page intentionally left blank**

TABLE OF CONTENTS

LIST OF FIGURES

R-1386

# ULTIMATE INTRINSIC-COERCIVITY SAMARIUM-COBALT MAGNET

## AN EARTH-BASED FEASIBILITY STUDY FOR SPACE-SHUTTLE MISSIONS

## 1. INTRODUCTION

High-performance samarium-cobalt magnets, produced by powder metallurgical processes, have now been on the scene for about a decade.[1]* The maximum energy products, $(BH)_{max}$, in these magnets have always been quite close to the maximum attainable for the alloy $SmCo_5$. The intrinsic coercivity, $H_{ci}$, in the early magnets ranged up to 25 kOe. Although this was an order of magnitude improvement over those of the existing commercial magnets at the time (except for Pt-Co magnets), it was only about a tenth of the theoretical maximum of 350 kOe.

The past 10 years have seen considerable studies by many researchers on this magnet material bringing about further improvement in the energy product and minor improvement in the intrinsic coercivity. It is possible to obtain $SmCo_5$ magnets from commercial sources with $H_{ci}$ value as high as 30 kOe. Here at The Charles Stark Draper Laboratory, Inc. (CSDL), we have produced sintered magnets with intrinsic coercivities reaching 42 kOe[2] and arc-plasma-sprayed (APS) magnets with intrinsic coercivities as high as 70 kOe.[3]

The theoretical maximum value of intrinsic coercivity is derived from the magnetocrystalline anisotropy of the $SmCo_5$ crystal. The saturation magnetization ($4\pi M_s$) along easy magnetization direction (c-axis) is reached at low magnetization fields of less than 10 kOe. However, it requires around 350 kOe to attain the saturation value when

---

* Superscript numerals refer to similarly numbered items in the List of References.

the magnetization field is applied in any direction in the plane perpendicular to the c-axis. The 350 kOe field required for saturation in the hard directions, known as the anisotropy field ($H_A$) is the maximum theoretical value of the $H_{ci}$. In other words, once the magnet is magnetized in a given easy direction, it should require a reverse field equal in magnitude to the value of $H_A$ to initiate and complete the reversal of magnetization, if no other mechanism of reversal were present.

Magnetization reversal in $SmCo_5$ magnets has been found to result from nucleation and motion of reverse magnetic domains. This is believed to be associated with the presence of defect sites in the conventionally prepared $SmCo_5$ magnets. Many of these defects are believed to be compositional inhomogeneities resulting from precipitation of dissolved oxygen during the cooling of the magnet from sintering and optimization temperatures.[4,5,6] In the conventional processes of preparing these magnets it is nearly impossible to maintain an oxygen-content level at less than 0.6 weight percent. With less than utmost care, the level goes up to 1.0 weight percent or even higher. Because of the high chemical reactivity of the element samarium, other contaminants also enter the alloy from the crucible materials in which the $SmCo_5$ alloys are melted. These other contaminants are also suspected to be contributors to undesirable defects.

## 2. OBJECTIVE

The objective of this research program is to demonstrate by ground-based experiments that it may be feasible to produce an intrinsic coercivity in a $SmCo_5$ magnet approaching its theoretical limit of 350 kOe as compared to the best achieved-to-date value of ~70 kOe at CSDL. To achieve this goal, the experimental efforts are directed towards elimination of contamination (particularly oxygen) from the finished magnet.

## 3. TASK DESCRIPTION

Basically, the program is envisioned as comprising of two main tasks.

(1) To produce contamination-free alloys of desired composition from pure elements, samarium and cobalt.

(2) To produce fine powder from these alloys and densify the powder without adding any contamination during processing, while retaining a fine-grained structure in the densified body.

The first task is being performed in existing electromagnetic levitation facilities at the Space Sciences Laboratory of the General Electric Company. Modifications will be introduced if they are deemed necessary. The second task will require facilities which would provide an ultra-pure atmosphere in which powder preparation, manipulation, and encapsulation of the powder will be carried out. The densification of the powder will be performed while still encapsulated without exposing the powder to any contaminating atmosphere.

A milestone chart showing the various details for carrying out the program is given in Appendix A. The program will require a period of 3 years and is divided into two phases with a 6-month overlap between phases 1 and 2. The task of major importance for the first phase is alloy-melting and for the second phase will be comminution and densification.

## 4. ELECTROMAGNETIC LEVITATION MELTING OF Sm-Co ALLOYS

### 4.1 Introduction

The work described here concerns the General Electric Task to develop a containerless reaction method for samarium-cobalt magnet materials. The objectives of this study are as follows.

(1) Reaction of pure Sm and Co to form pure $SmCo_5$.

(2) Avoidance of contamination from crucible or from coolant gas.

Previous experiments[7,8] in reaction of Sm and Co in crucibles or by plasma arc or induction heating show contamination due to oxygen or aluminum pickup. $SmCo_5$ reacts with all known crucible materials such as pyrolytic BN.

To eliminate these problems, the proposed solution is a containerless reaction using electromagnetic levitation terrestrially or in a weightless space environment.[7]

In the following, the experimental work from the beginning of October 1979 through the end of February 1980 will be briefly presented. The bulk of the experimental work performed was directed towards the aforementioned objectives. The objectives have not yet been completely met. Additional experimental work is needed to fully evaluate the potential of this new process.

## 4.2 Experimental Methods and Results

The electron beam heating and levitation facility (~4 kW maximum beam power input; 450 kHz, 25 kW RF power generator) were repaired and reactivated. Elemental samarium and cobalt were obtained as well as samarium-cobalt alloy for the experiments. Although considered initially, early analysis of the samarium evaporation rate at the required reaction temperatures showed that electron beam gun poisoning or shut-down from arcing could not be avoided with available pumping arrangements.

At the beginning, the characteristics of RF heating of the materials were explored. RF heating of the alloy on a boron nitride pedestal led to arcing problems, despite the use of a slow temperature rise. Melting of the alloy in a cobalt crucible by RF heating in an argon atmosphere showed that the reaction with the crucible material is so rapid that adequately prompt termination of reactions carried out on a pedestal which avoids contamination from foreign materials will be difficult and probably impossible.

Therefore, the work performed was aimed at developing a suitable technique for reaction of elemental cobalt and samarium, which would avoid crucible or pedestal contamination. A radiation pyrometer was assembled by using optical filters and an available GE Charge Injection Device (CID) imager. A new RF coil suitable for better containment was fabricated and tested. Also, a new gas injection device was installed for cooling the levitated melt. A schematic sketch of the levitation and gas-cooling facility is shown in Figure 1.

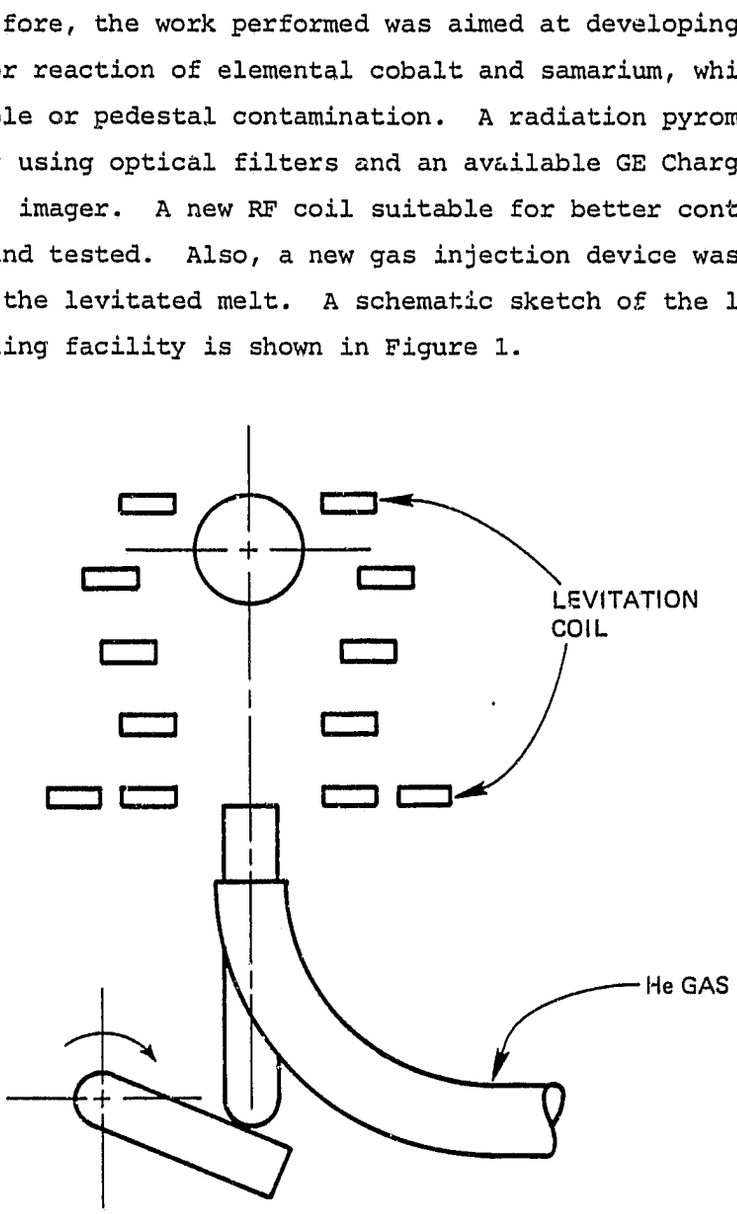


Figure 1. Electromagnetic levitation and gas-cooling provisions.

Pyrometer calibration is mandatory to provide accurate temperature readings. It was performed by viewing alternatively the smooth surface of cobalt and a nearby deep-drilled cavity in the specimen,

which simulated a black body at the same temperature. Gold (melting point 1336 K) and constantan (melting point 1543 K) wires were used for absolute calibration. A sketch of the equipment is depicted in Figure 2. The developed instrumentation also allowed measurement of normal emissivity of cobalt by comparison of the radiation from the cavity drilled in the specimen to the intensity of radiation emitted from the exposed cobalt surface just beside the cavity. Values obtained were 0.69, 0.72 ± 0.04 and 0.85 at 1336, 1543 and 1768 K, respectively. These temperatures were established by observing the melting of gold, constantan and cobalt. These values apply at 0.85 and 0.65 micrometers. The techniques are thus in hand for controlling reaction temperatures for compacts of elemental samarium and cobalt where a containing cobalt jacket is used, at least up to the point where the outer surface of the capsule participates in the reaction.

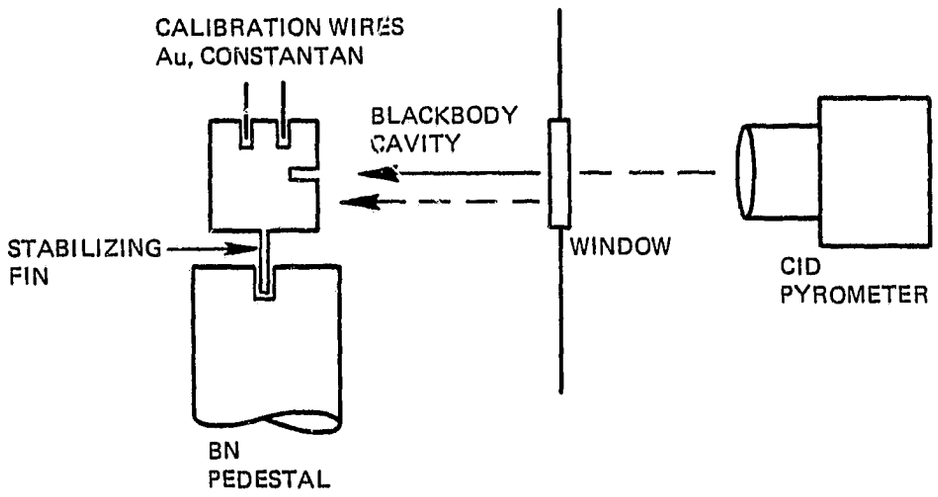


Figure 2. Emissivity measurement.

A cobalt ball (1 cm dia.) was used to simulate the heating and cooling of samarium-cobalt alloy, while at the same time allowing emissivity, and hence temperature determinations. Because of the near

equality of the density of Co and $SmCo_5$, it was expected and later verified that the observed solidification of the levitated Co which was achieved can be repeated with $SmCo_5$. In the course of experiments, helium gas played the major role in cooling and solidifying the cobalt.

Experiments on melting and solidification of pure cobalt allowed determination of optimum levitation position, levitation power, and helium coolant flow to obtain various temperatures in the neighborhood of 1400 to 1500 K where the samarium-cobalt reaction should be carried out so as to avoid excessive vaporization loss of the samarium. Gas velocities of the order of 30 meters per second or greater are required to achieve solidification. At these velocities, aerodynamic levitation forces become appreciable so that there is interaction between the electromagnetic and aerodynamic levitation. Figure 3 shows the exterior of a typical cobalt specimen after solidification. A pyrometer trace is shown in Figure 4 for the heating and cooling curve for this cobalt levitation experiment.

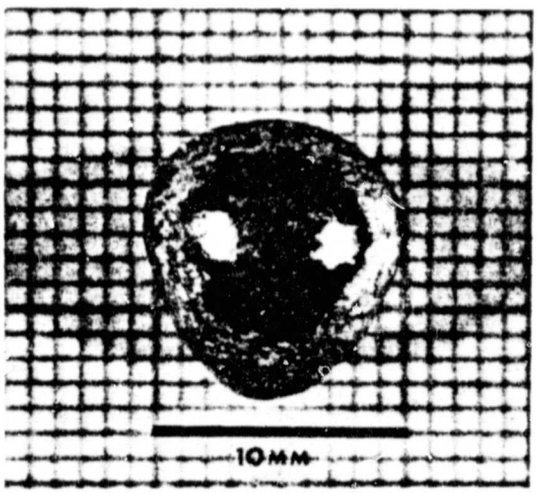


Figure 3. Exterior of cobalt after solidification.

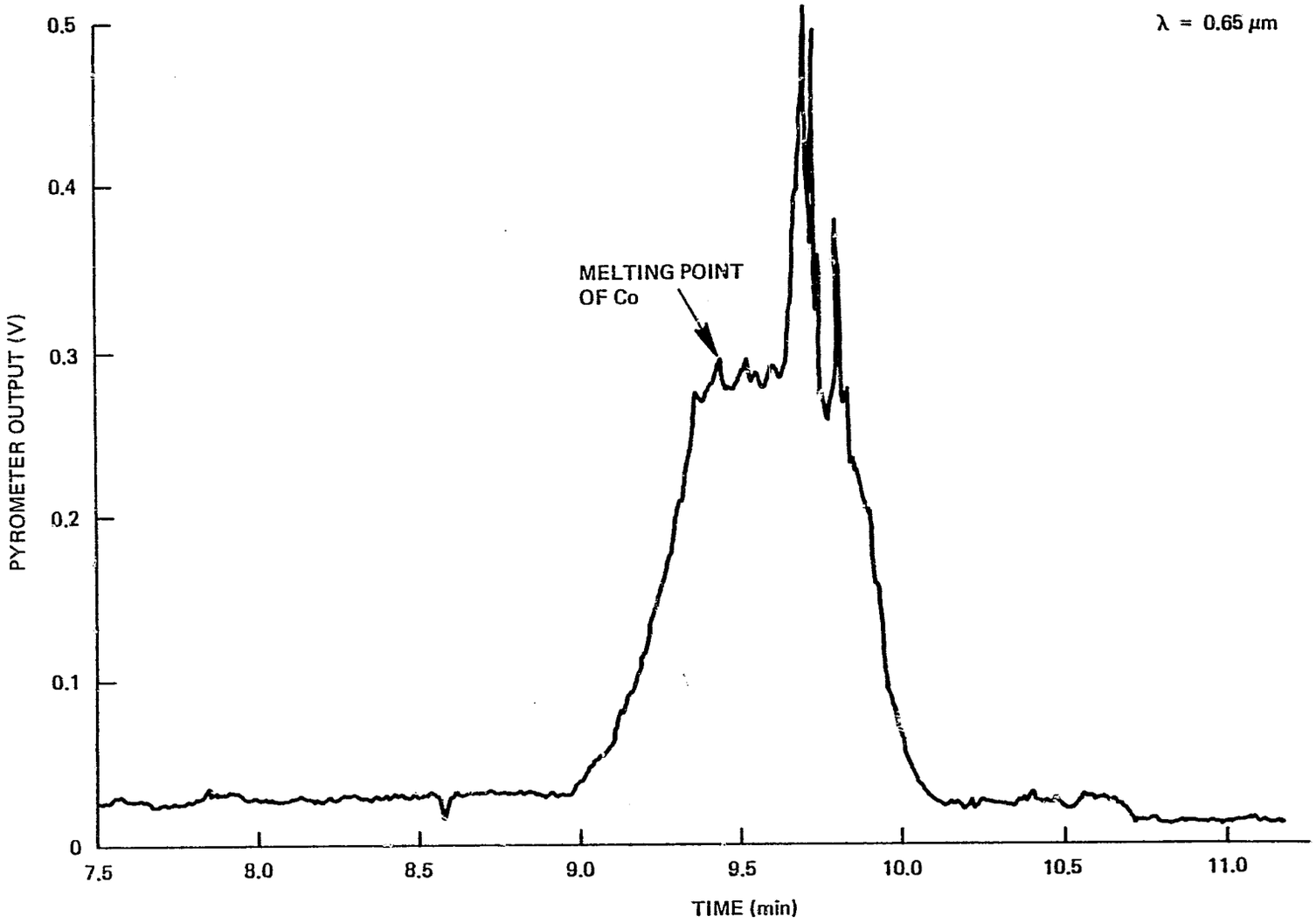


Figure 4. Pyrometer trace for heating and cooling curve of cobalt levitation experiment.

Experiments were carried out on levitation melting and solidification of samarium-cobalt alloys (#1208, 34.3 percent of Sm) furnished by CSDL to assess problems of samarium evaporation and oxidation from residual oxygen or water vapor in the helium coolant stream. Initial experiments with the helium coolant caused sufficient oxide to form on the surface of the samarium-cobalt that a shape change was not observed upon melting. A helium scrubber, as shown in Figure 5, was constructed and placed in operation which is capable of removing the major part of the oxygen and water vapor contaminant by passing the gas sequentially through a liquid nitrogen trap and through copper screens heated to 600°C in an oven. This allowed a major reduction in the oxidation of the melt surface, as evidenced by the easy subsequent observation of the shape change upon melting and the very thin layer of oxide observed on the solidified specimen.

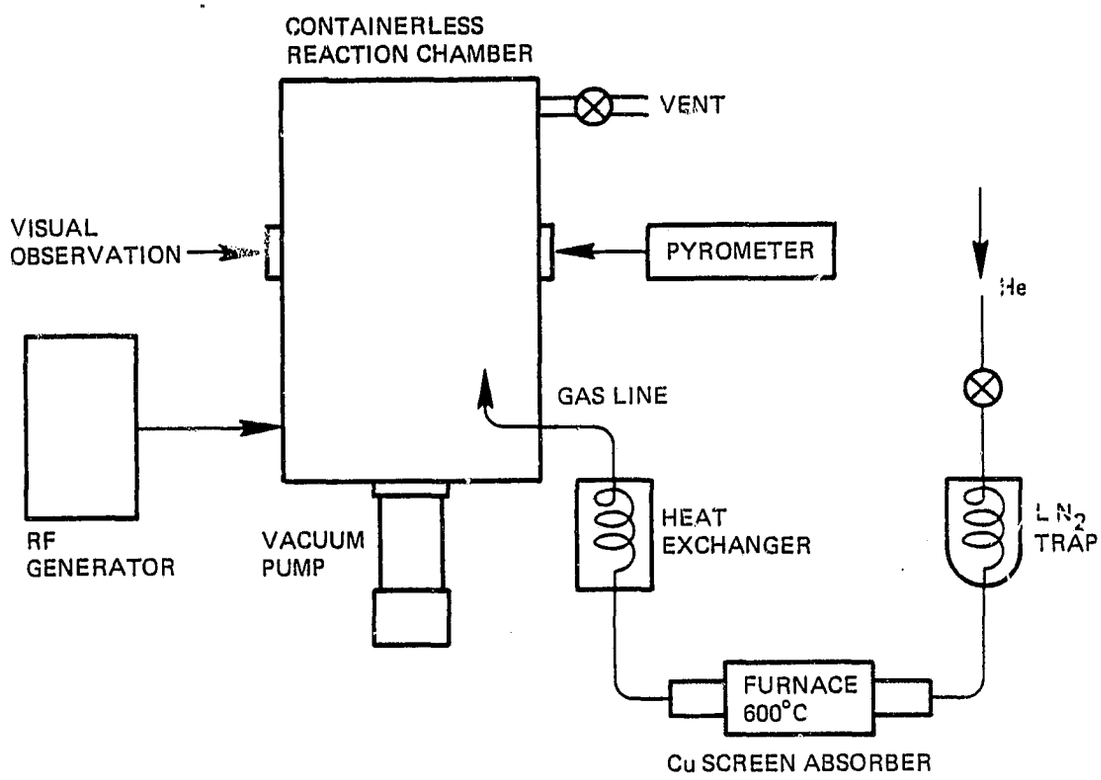


Figure 5. Samarium-cobalt reaction experiment.

The external surface of a levitated specimen of samarium-cobalt alloy after solidification is shown in Figure 6. Figure 7 shows the heating and cooling curve for the same specimen from the output of the radiation pyrometer. For this experiment, in which the best temperature control was achieved, a weight loss of 72 milligrams of samarium out of a total of 1.2 grams was measured. The corresponding evaporation rate of samarium is approximately $1.8 \times 10^{-3}$ g/cm$^2$ s. This agrees roughly with calculations based on published vapor pressure data for pure samarium as discussed in the following.

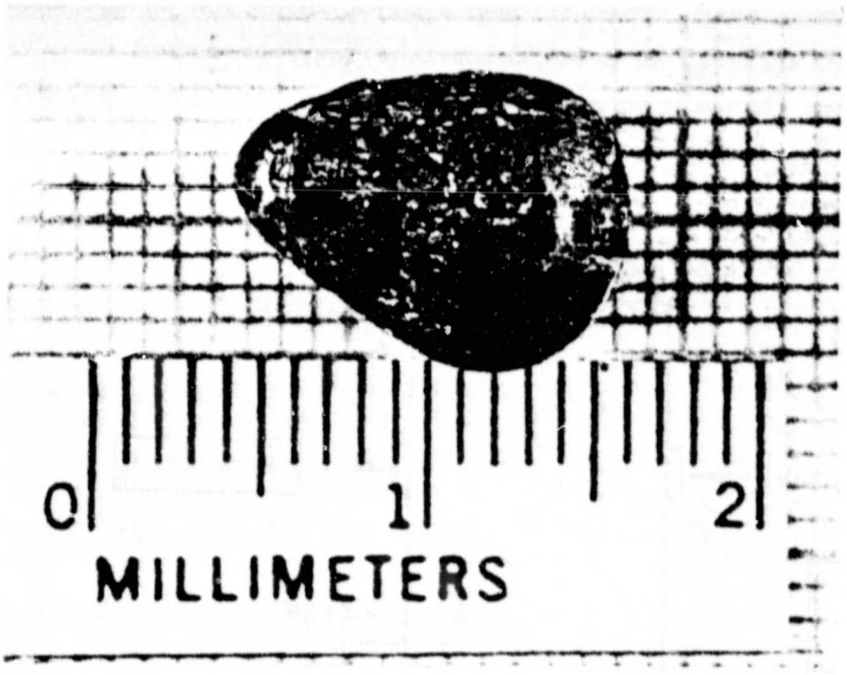


Figure 6. External surface of levitated samarium-cobalt specimen after solidification.

A preliminary attempt to levitation melt pure samarium was unsuccessful because of excessive heating of the material before it could be levitated.

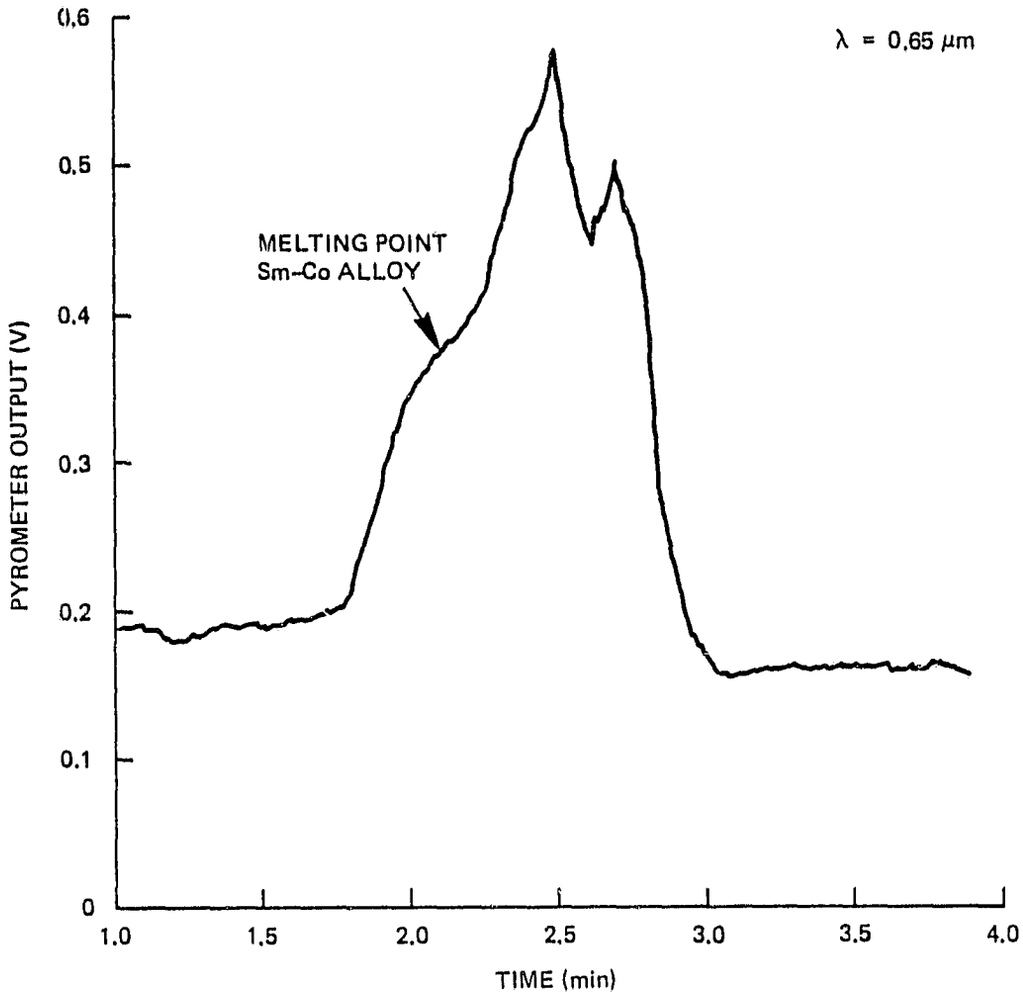


Figure 7. Heating and cooling curve for levitated samarium-cobalt specimen from the output of the radiation pyrometer.

The experimental sequence is briefly summarized as follows.

(1) Induction melting of Sm-Co charges on a BN pedestal and on a Co crucible.

(2) Pyrometer calibrations for known melting points of Au, constantan, and Co, and emissivity measurement for Co.

(3) RF levitation melting and He-cooled solidification of Co.

(4) Levitation melting and solidification of Sm-Co alloy with the scrubber.

## 4.3 Analysis and Discussion of Results

The experimental results will be briefly discussed and analyzed in terms of the first principle wherever possible. The detailed descriptions and notations used will be presented in the final report.

### 4.3.1 Error Analysis On Emissivity Measurement for Co

From the error of measured emissivity, we can estimate the temperature deviation corresponding to the estimated experimental error in measurement of the emissivity as

$$\frac{\Delta T}{T} \sim \frac{1}{4} \frac{\Delta \varepsilon}{\varepsilon} \tag{1}$$

For T = 1500 K, $\Delta\varepsilon/\varepsilon$ is 0.04/0.72. Thus, we obtain

$$\Delta T = \pm 21 \text{ K}$$

### 4.3.2 Electromagnetic and Aerodynamic Levitation

The approximate formula for the electromagnetic levitation force acting on the specimen is[9]

$$F = -\frac{a^3}{4} G(x) \text{ grad } B^2 \tag{2}$$

where x is $a/\delta$ and G is a function well known in the levitation literature.[3] $\delta$ is the electromagnetic skin depth.

For a flow around a sphere, the aerodynamic levitation force can be correlated by the following formula[4]

$$F_K = (\pi a^2)(\frac{1}{2}\rho v_\infty^2) f \tag{3}$$

where f is known as the friction factor.

To levitate a cobalt ball (1 cm dia.) aerodynamically, the required minimum free-stream velocity of helium is around 120 m/s. For gas velocity of 30 m/s, the force due to aerodynamic levitation is around 6 percent of total levitation force.

### 4.3.3 Heating Due To Electromagnetic Levitation and Heat Removal By Forced Convection

The resultant joule heating due to electromagnetic levitation is approximately[3]

$$N = \frac{3 \cdot 10^9}{16\pi} a\rho_e F_1(x) B^2 \qquad (4)$$

where $F_1(x)$ is another function of x widely used in the analysis[9] of levitation experiments.

The power absorbed by a levitated $SmCo_5$ ball (1 cm dia.) is around 130 watts. The radiated power at 1200°C and emissivity 0.8 is 66 watts. Thus, the heat required to be removed by gas streams will be 64 watts.

For flow around a sphere, the following equation may be used for heat transfer calculation[10]

$$Nu = 2.0 + 0.6\ Re^{1/2}\ Pr^{1/3} \qquad (5)$$

To remove 64 watts heat by helium gas at room temperature, the computed free-stream velocity is around 30 m/s. This result is very close to the experimental value mentioned previously.

### 4.3.4 The Evaporation Rate of Samarium

The maximum rate at which molecules of a vapor can leave the surface of a liquid during evaporation in vacuum is given by Langmuir[11]

$$j_A = 5.833 \times 10^{-2} P_v \left(\frac{M_A}{T}\right)^{1/2} \quad (6)$$

According to the Maxwell-Stefan law of molecular diffusion, the rate of diffusion of the vapor A through a residual gas B is given as follows[4]

$$j_A = \frac{PD_{AB}M_A/RT}{\delta} \ln \frac{P_{B_2}}{P_{B_1}} \quad (7)$$

This equation indicates the possible effect of the inert gas on the rate of evaporation of the liquid. The theory has been verified by an experimental study investigated by Wu et al.[12] This fact also suggests an additional rationale for possible weightless environment performance samarium-cobalt experiments as discussed in the following.

Equation (7) also finds use in the film theory[10] of mass transfer. In this model it is assumed that there is a sharp transition between a stagnant film and a well mixed fluid in which concentration gradients are negligible. From the boundary layer theory, $\delta$ can be estimated as follows[13]

$$\delta \sim \frac{\nu x}{v_\infty} \quad (8)$$

Furthermore, the correlation of Ranz and Marshall[10] may be used for mass transfer calculation for forced convection around a sphere

$$Sh = 2.0 + 0.6\, Re^{1/2}\, Sc^{1/3} \quad (9)$$

In this study, samarium-cobalt alloy was heated to 1500°C and then solidified. The theoretical results based on Langmuir model, film

theory, and Ranz and Marshall model are 1.7, $2.0 \times 10^{-3}$, and $6.0 \times 10^{-3}$ $g/cm^2$ s, respectively. The last two values compare reasonably well with the experimental result mentioned previously.

## 4.4 Conclusions and Recommendations for Future Work

An important first objective of the program has now been met with the successful development of techniques for containerless melting and solidification of the compound without excessive oxidation. Initiation of the experiments to levitate samarium contained in a cobalt capsule will be initiated as soon as additional funding becomes available.

In light of the experiments carried out to date, it is now realized that the high evaporation rate of Sm is due to the high velocity of the coolant gas. This constitutes an additional rationale for possible experiments in a weightless environment where a quiescent coolant gas could be used since RF induction heating could be adjusted to a value to obtain the desired specimen temperature and resultant reaction rate. The earlier rationale mentioned in the proposal[7] for this work failed to recognize the deleterious effect of rapidly flowing gas as required in the terrestrial experiments in terms of samarium loss and consequent effect on stoichiometry.

Finally the improvements in techniques expected in microgravity experiments are summarized as follows.

(1) Precise control of temperature by setting of RF power to a level dictated by pyrometer reading.

(2) Elimination of temperature surge due to settling of levitated charge upon melting.

(3) Provision of quiescent gas envelope to inhibit Sm evaporation instead of promotion of evaporation from rapid removal of gas film by rapidly moving gas.

(4) Ability to search for a possible suspected phase change in free-cooling melt.

In a recent meeting of the NASA Containerless Processing Task Team[14] considerable attention was given to the possibility for performing certain simple experiments in the SPAR rocket version of an electromagnetic containerless processing device.[15] A recommendation was made that NASA consider refurbishing this apparatus, which has already been successfully flown aboard a rocket, for free-cooling experiments for pure materials in order to explore further the technique for thermodynamic property measurements by free-cooling experiments. Other suggestions were made for experiments in undercooling in the quiescent environment available to a containerless liquid metal in the weightless environment. Very limited attention was given to a proposal that a similar experiment for free cooling of molten samarium-cobalt would be very useful to help resolve objective (4) previously listed. From the aforementioned recently obtained results on the deleterious promotion of samarium vaporization in the ground-based containerless reaction experiments, even if such a reaction can be carried out successfully terrestrially, it already appears that some consideration should be given to extending the present containerless reaction experiments in the weightless environment. An important circumstance is that the expected optimum reaction temperature in the neighborhood of 1200 to 1300°C is easily within the capability of the apparatus developed for SPAR.

## 5. EXAMINATION OF RELATIONSHIP BETWEEN COERCIVITY AND $O_2$ CONTENT IN APS MAGNETS

### 5.1 Experiments and Results

Arc-plasma-sprayed $SmCo_5$ magnets produced at CSDL recently had intrinsic coercivities in the range of 70 kOe. These high values of coercivities were obtained in magnets with oxygen content of about 0.15 weight percent. As mentioned already, the sintered magnets can be produced with a minimum oxygen content of 0.6 weight percent. The comparatively lower level of oxygen content in APS magnets gave us an opportunity to examine the effects of oxygen content in the range 0.15 to 0.6

weight percent on the coercivity of the magnet. The investigations were carried out by deliberately increasing the amount of oxygen in the APS magnet, by controlled low-temperature oxidation of the spray powder.

An alloy of Sm-Co with a composition of 41.8 percent Sm was ground and the desired sieving fraction was selectively oxidized. Oxygen content of the alloy powder was found to be 0.19 weight percent before oxidation. After oxidation, samples from various batches of oxidized powder were also analyzed. Based on the measured oxygen value, each batch was then blended with Sm-Co alloy powder containing 46 weight percent Sm and 0.113 weight percent $O_2$ to restore the metallic Sm content to 41.2 weight percent. The oxygen content of the blended powders were recalculated. The sprayed deposits were once again analyzed for oxygen. Since the oxygen content in the sprayed samples was found to be considerably higher in the sprayed deposits than in the powders, the Sm content of the spray powders was recalculated. All of this is shown in Table 1. The new calculated amounts of Sm were close to being the desired amounts, although somewhat on the low side in samples A, B, D, and I. Samples C, E, and H were much too low in Sm content, and it would be impossible for them to produce $SmCo_5$ in the deposit. The above observations were confirmed by X-ray diffraction patterns taken on some selected spray deposits shown in Table 1.

From the APS deposits, measurement specimens were prepared by the electrodischarge-machining process. The dimensions used were 0.200 inch. diameter by approximately 1/16 inch thick. The specimens were heat treated at successively higher temperatures. Magnetic measurements were performed after each heat treatment in order to determine the change in coercivities due to the increase in grain size. The results of these measurements are shown in Table 2.

Table 1. Measured and calculated $O_2$ and Sm contents and X-ray diffraction structures.

| Sample No. | wt % $O_2$ Before Blending (Measured) | wt % $O_2$ After Blending (Calculated) | wt % $O_2$ After Spraying (Measured) | Recalculated wt % Sm in Starting Powder | X-ray Diffraction of Sprayed Sample |
|---|---|---|---|---|---|
| A (unoxidized) | 0.19 | 0.18 | 0.38 | 40.0 | $SmCo_5$ |
| B | 0.56 | 0.39 | 0.45 | 39.6 | $SmCo_5$ |
| C | 1.14 | 0.53 | 5.2 | 12.9 | $Sm_2Co_{17}$ - weak<br>Co - Strong |
| D | 0.59 | 0.40 | 0.49 | 40.5 | $SmCo_5$ |
| E | 2.81 | 0.67 | 3.3 | 25.5 | $Sm_2Co_{17}$ - strong<br>Co - Weak |
| H | 2.73 | 0.67 | 3.5 | 24.1 | — |
| I | 0.87 | 0.48 | 0.63 | 40.2 | — |

Table 2. Coercivities $H_{ci}$* and $H_K$** of APS magnets after various thermal treatments.

| Thermal Treatment | | 1000°C - 2 h 900°C - 3 h Quick Cooled (1) | | 1000°C - 2 h 900°C - 3 h Furnace Cooled (2) | | 1108°C - 3 h 900°C - 24 h Quick Cooled (3) | | 1140°C - 17 h 900°C - 32 h Quick Cooled (4) | |
|---|---|---|---|---|---|---|---|---|---|
| Sample No. | wt % Oxygen | $H_{ci}$ (kOe) | $H_K$ (kOe) | $H_{ci}$-kOe | $H_K$-kOe | $H_{ci}$-kOe | $H_K$-kOe | $H_{ci}$-kOe | $H_K$-kOe |
| A | 0.38 | 57 | 20 | 32 | 12 | 56 | 28 | 55 | 33 |
| B | 0.45 | 59 | 23 | 33 | 12 | 63 | 25 | 64 | 27 |
| D | 0.49 | 64 | 23 | 60 | 21 | 63 | 25 | 65 | 29 |
| I | 0.63 | 57 | 9 | 31 | 7 | 57 | 9 | 51 | 10 |
| X | 0.15 | 70 | 33 | 70 | 33 | — | — | — | — |

* $H_{ci}$ = Intrinsic Coercive Force

** $H_K$ = Reverse Field at which 90% of original induction is retained.

Note: The results of samples C, E, and H are not shown in the above table, because the coercivities in these samples were less than 1 kOe, which was also expected on the basis of their chemistry.

Microstructures of the APS samples were examined after various thermal treatments. Optical micrographs of a number of samples are shown in Figures 8 through 12 at 500× magnification. The etchant used was 3 percent nital, which is very effective in revealing the phase compositions in Sm-Co alloys. A fairly good delineation of the individual grains is brought out by this etchant, although there are better etchants for this purpose.

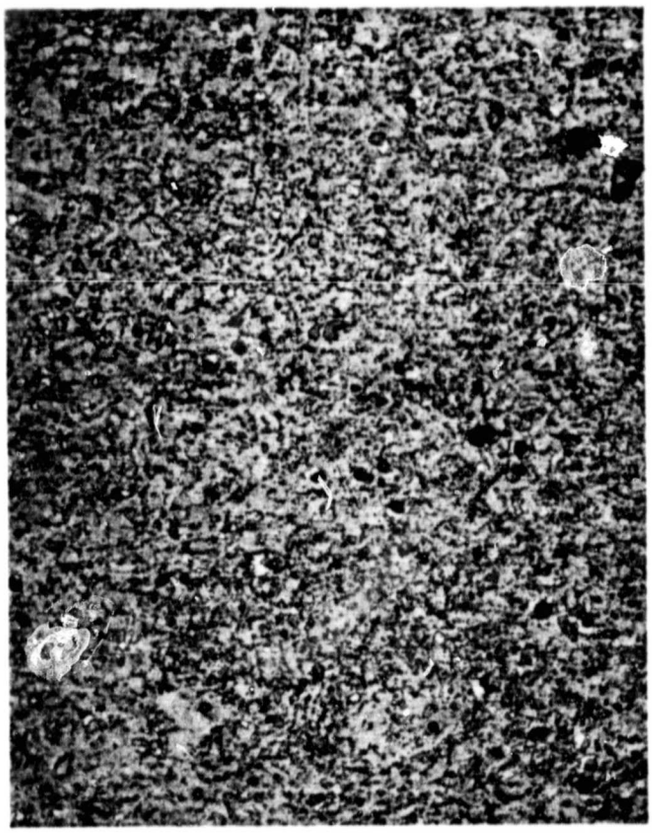

Figure 8. Sample A after heat treatment of 1140°C - 3 h, 900°C - 24 h, quick-cooled (mag. 500×).

Figure 9. Sample B after heat treatment of 1108°C - 3 h, 900°C - 24 h, quick-cooled (mag. 500×).

Figure 10. Sample D, after heat treatment of 1108°C - 3 h, 900°C - 24 h, quick-cooled (mag. 500×).

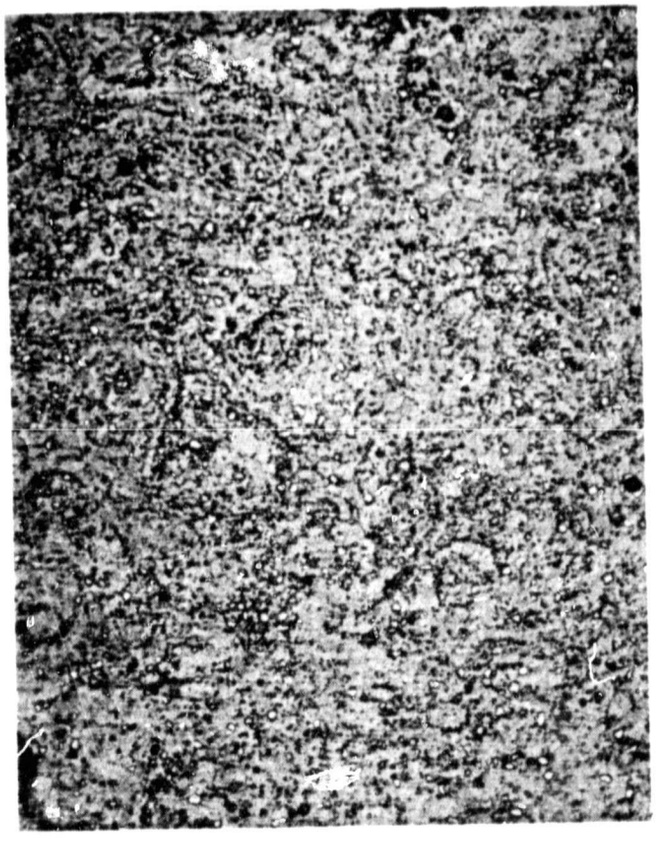

Figure 11. Sample I, after heat treatment of 1108°C - 3 h, 900°C - 24 h, quick-cooled (mag. 500×).

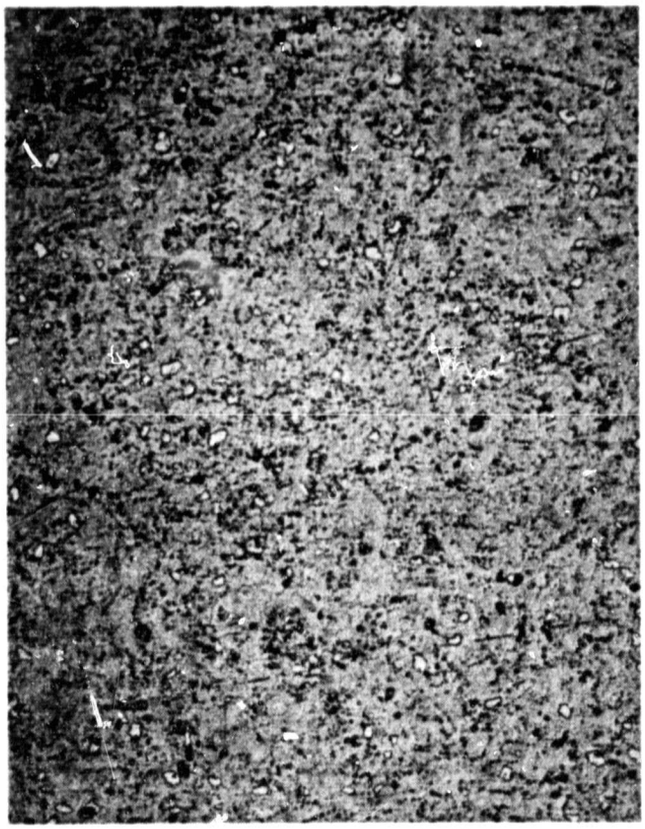

Figure 12. Sample I, after heat treatment of 1140°C - 17 h, 900°C - 24 h, quick-cooled (mag. 500×).

## 5.2 Discussion

The discrepancy in the oxygen analyses of the oxidized powder and the sprayed samples can only be explained as poor sampling of the oxidized powder batches. The oxygen analysis obtained on the spray samples are much more reliable, because the calculated amount of metallic Sm on the basis of these determinations are supported both by the phase compositions seen in the microstructures as well as by X-ray diffraction analysis.

The APS magnets are known to have grain sizes in the range of 2 to 5 micrometers after the 1000°C treatment. These samples showed coercivity as to be expected in columns (1) and (2) of Table 2. All the furnace-cooled samples had lower coercivity due to precipitation of $Sm_2O_3$ and formation of $Sm_2Co_{17}$ defects, except for sample D which retained its coercivity through the furnace cooling. This behavior of sample D is associated with much lower oxygen content than D had. For comparison, we have included an earlier sample designated 'X', for which furnace cooling had no damaging effect. The behavior of the furnace-cooled sample D is not explainable at this time.

The higher temperature treatments, given the present APS samples, produced somewhat larger grain sizes, but not as large as we had expected. Figure 9, 10, and 11 show the grain sizes of around 5 micrometers average in samples B, D, and I after a heat treatment at 1108°C. Samples B and I (Figure 9 and 11) show some fine $Sm_2Co_{17}$ grains (very light color). Sample D, having a larger Sm content, shows no $Sm_2Co_{17}$. Figure 8 is the microstructure of sample A after a thermal treatment of 3 hours at 1140°C. This shows clusters of extremely fine grains of $Sm_2Co_{17}$, and an average grain size of about 10 micrometers. Figure 12 is the microstructure of sample I after an extended treatment of 17 hours at 1140°C. The grain sizes (5 to 10 micrometers) in this sample are more or less of the same dimensions as in sample A in Figure 8. A very interesting comparison can be seen in Figure 11 and 12 for the sample I treated at 1108°C and 1140°C. Not only have the $SmCo_5$ grains increased in size, but larger number of

finer grains of $Sm_2Co_{17}$ are now replaced by a smaller number of coarser particles. In neither case was there any damage to the coercivities. This corroborates a recent publication by the authors[16] that as long as the $Sm_2Co_{17}$ particles are discrete they do not have adverse effects on coercivity.

Although our present experiments with the APS magnets failed to provide us with extemely large grain sizes of 30 micrometers or so as encountered in normal sintered magnets, we did cover a range of grain sizes between 2 to about 10 micrometers. In the range of grain sizes we produced, we saw an increase of coercivity with increasing grain size. This is contrary to normal expectations. There are factors involved which we are unable to explain at the present time.

The purpose of undertaking this investigation was to examine the relationship of coercivity to oxygen content in the range of 0.15 to 0.6 weight percent and higher. In this range of oxygen content, grain size along with the compositional chemistry, it is believed, played a more important role. More meaningful studies will come when we are able to lower the oxygen content to less than 0.1 weight percent. Just to have an idea of how enormous an amount of oxygen 0.1 weight percent is, we carried out some simple calculations and determined that a 5-micrometer cube of $SmCo_5$ particle with 0.1 weight percent $O_2$ would contain approximately $4 \times 10^{10}$ atoms of oxygen. That number of oxygen atoms could conceivably generate numerous defect sites of $Sm_2Co_{17}$ in the $SmCo_5$ grain, any one of which could cause reversal of magnetization at comparatively low reversing fields. Of course, the solubility value of oxygen at room temperature is not known, although we expect it to be a finite value. Whatever amount of oxygen remains in solution without the tendency to precipitate will do no more damage magnetically than to lower the magnetocrystalline anisotropy somewhat, and do a similar amount of damage to the anisotropy field which is the theoretical maximum of intrinsic coercivity. Until we develop methods to reduce the oxygen content in those ranges, meaningful relationships between oxygen content and coercivity can not be determined.

## 5.3 Conclusions and Future Plans

The present study to examine the effect of oxygen content on the coercivity of $SmCo_5$ magnets and, as a side issue, the effect of grain size was inconclusive. The range of oxygen content from 0.15 to 0.63 weight percent obviously would not permit a proper evaluation. In the range of grain size between about 2 and 10 micrometers, larger grain sizes did not appear to degrade the coercivity.

In order to determine the relationship between oxygen content and coercivity, we must be able to produce densified $SmCo_5$ magnets with oxygen content much less than 0.1 weight percent or the actual solubility of oxygen in the $SmCo_5$ lattice, whichever is smaller. As shown in the milestone chart in Appendix A, we shall now proceed to evaluate comminution and encapsulation techniques towards the goal of greatly reducing the amount of oxygen in the alloy powder. Our arc-plasma-spraying procedure as carried out now is not capable of reducing the oxygen content to less than about 0.15 weight percent.

The following are the major findings during this investigation.

(1) Sample B indicates that $Sm_2Co_{17}$ formation due to evaporation loss actually helps rather than damages the coercivity (possibly due to increased homogeneity within the grains).

(2) Grain size increase improves coercivity, also perhaps by producing higher degree of homogeneity.

(3) Oxygen plays a minor role in the range of 0.15 to 0.6 weight percent provided that adequate chemistry is maintained.

(4) Grain growth was substantially inhibited.

The findings will be the basis for a publication (perhaps in The Journal of Applied Physics) in the near future.

**Page intentionally left blank**

# APPENDIX A

## MILESTONE CHART

Program Milestone Chart (Sheet 1 of 3)

Marshall Space Flight Center, Materials Processing in Space Office, Experiment Development Office

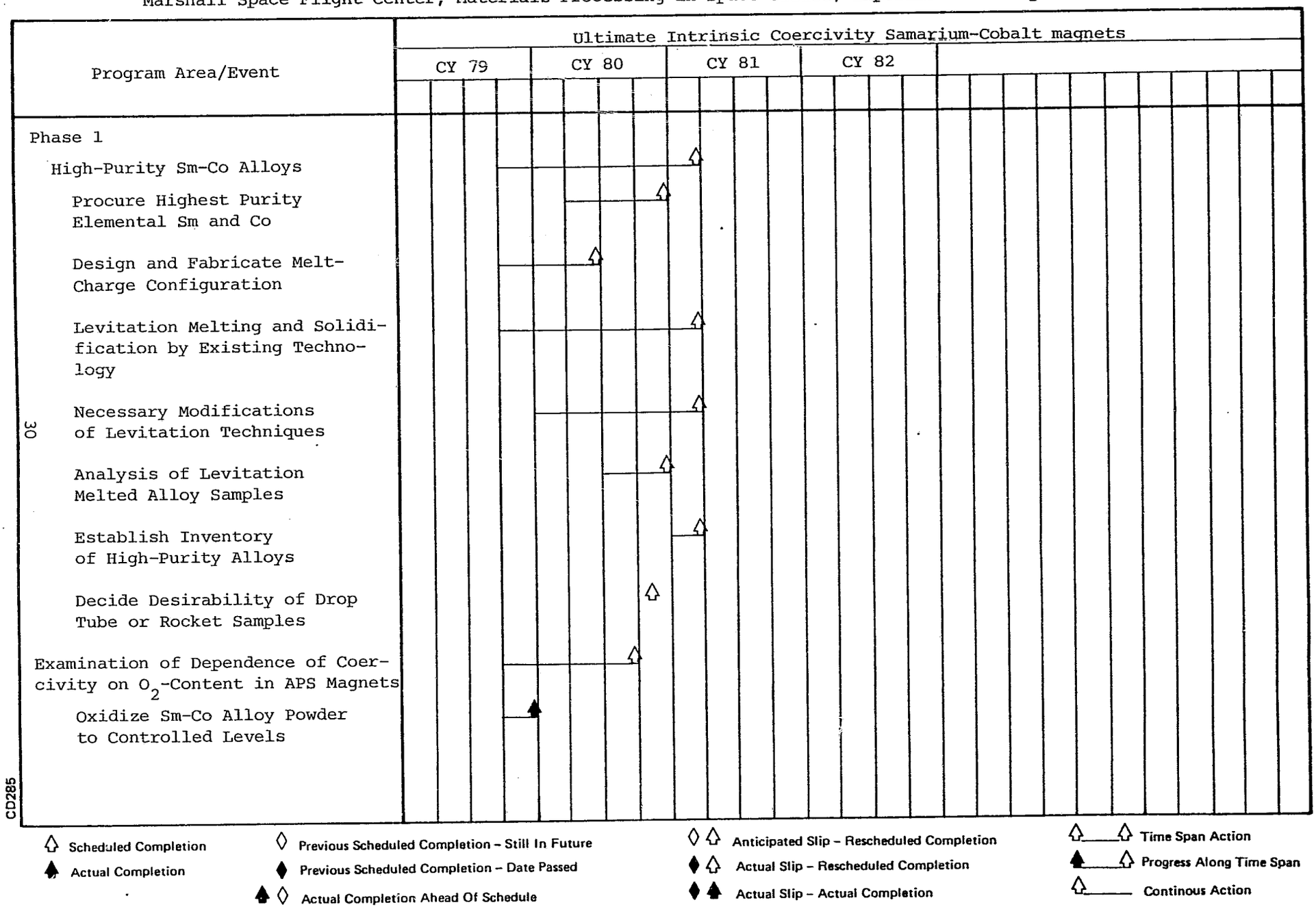




CD285

Program Milestone Chart (Sheet 2 of 3)

Marshall Space Flight Center, Materials Processing in Space Office, Experiment Development Office

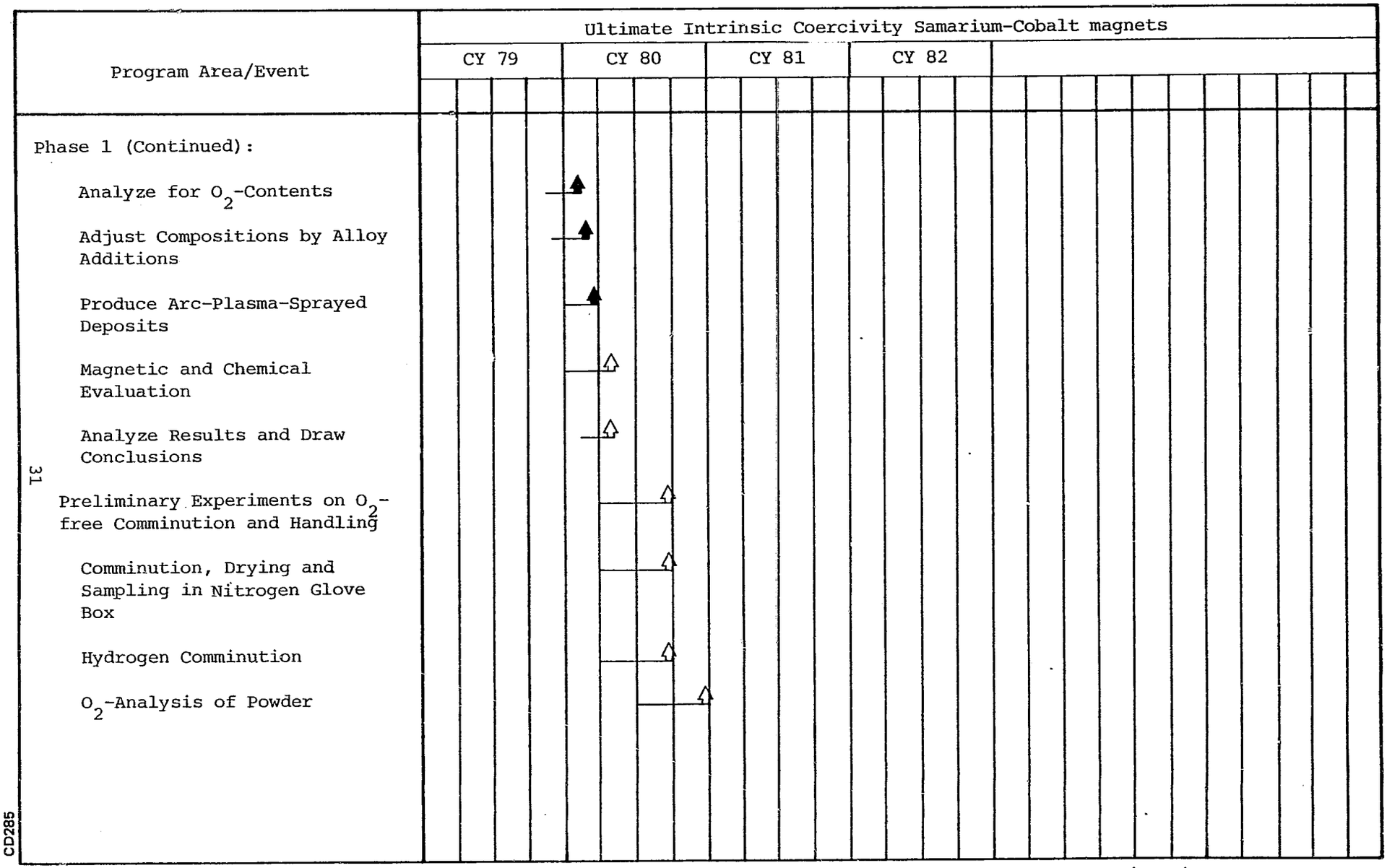




CD285

Program Milestone Chart (Sheet 3 of 3)

Marshall Space Flight Center, Materials Processing in Space Office, Experiment Development Office

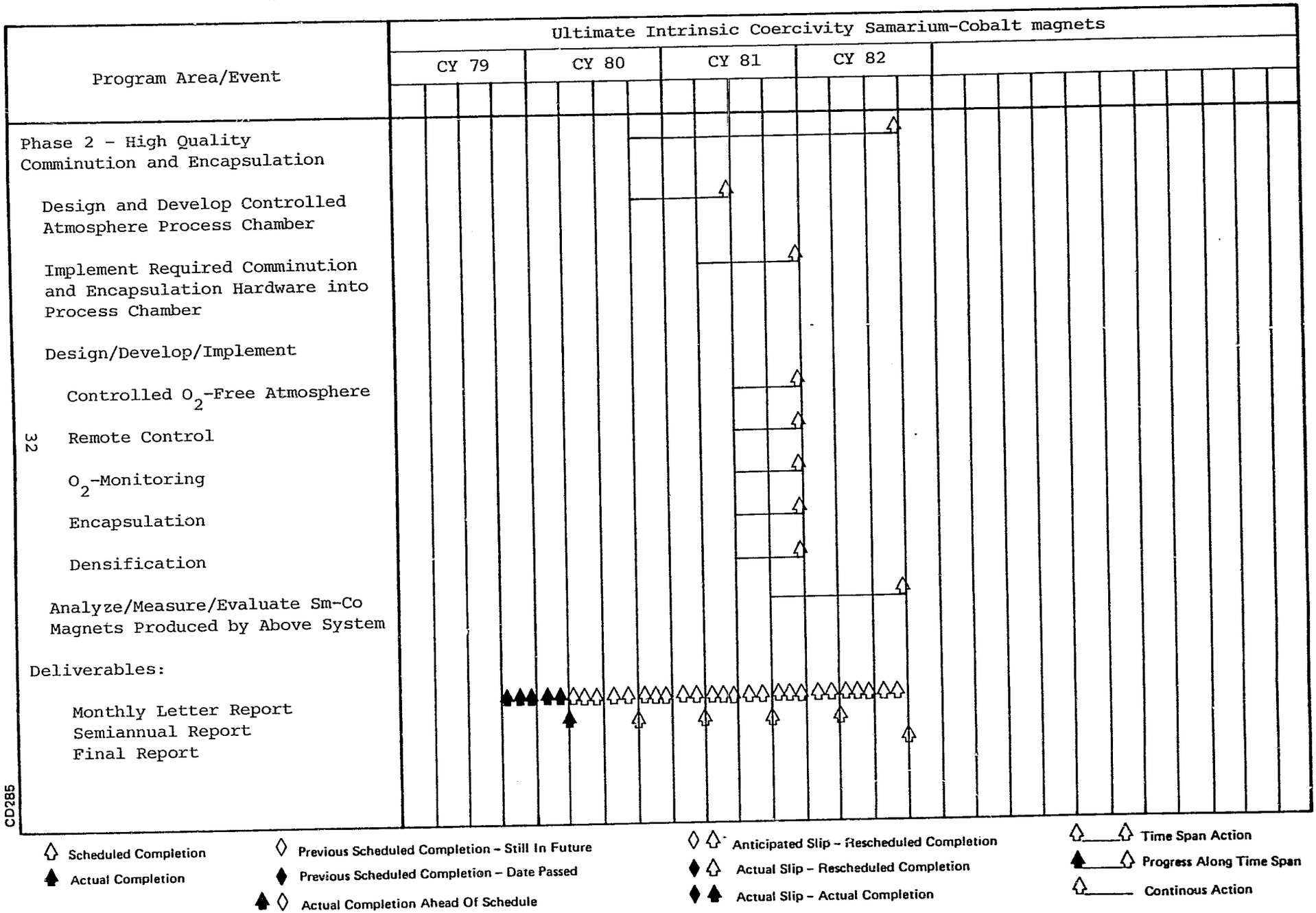

## LIST OF REFERENCES


1. Das, D., "Twenty Million Energy Product Samarium-Cobalt Magnet," IEEE Trans. Magnetics, MAG-5, No. 3, p. 214, September 1969.

2. Das, D., K. Kumar, and E. Wettstein, Rare Earth Magnetic Material Technology As Related to Gyro Torquers and Motors, Technical Report No. 2. Prepared for the Office of Naval Research, Under Contract N00014-77-C-0388, October 1979.

3. Kumar, K., D. Das, and E. Wettstein, "High Coercivity Isotropic Plasma Sprayed Samarium-Cobalt Magnets", J. Appl. Phys., 49, p. 2052, 1978.

4. Bartlett, R. W., and P. J. Jorgensen, "Microstructural Changes in $SmCo_5$ Caused by Oxygen Sinter-Annealing and Thermal Aging," J. Less Common Metals, 37, p. 21, 1974.

5. Das, D., and W. Harrold, "Characterization of Samarium-Cobalt TWT Magnets," IEEE Trans. Magnetics, MAG-7, No. 2, p. 281 June 1971.

6. Kumar, K., D. Das, and E. Wettstein, "Samarium-Cobalt Magnets Resistant to 750°C," IEEE Trans. Magnetics, MAG-14, p. 788, 1978.

7. Ultimate Intrinsic-Coercivity Samarium-Cobalt Magnet, An Earth-Based Feasibility Study for Space-Shuttle Missions, CSDL Proposal 8-792, April 1978.

LIST OF REFERENCES (Continued)


8. Miller, J. F., and A. E. Austin, "Container Materials for Molten $SmCo_5$," J. Less Common Metals, 25, p. 317, 1971.

9. Electromagnetic Containerless Processing Requirements and Recommended Facility Concept and Capabilities for Spacelab, Final Report NASA Contract NAS8-29680, 13 May 1974.

10. Bird, R. B., W. E. Stewart, and E. N. Lightfoot, Transport Phenomena, John Wiley & Sons, Inc., 1960.

11. Dushman, S., Scientific Foundations of Vacuum Technique, John Wiley & Sons, Inc., 1962, 2nd ed.

12. Wu, P. C. S., T. J. O'Keefe, and F. Kisslinger, "The Inert Gas Effect on the Rate of Evaporation of Zinc and Cadmium," Met. Trans. A, 11A, p. 123, 1980.

13. Schlichting, H., Boundary-Layer Theory, Pergamon Press, 1968, 6th ed.

14. Minutes of the Electromagnetic Containerless Processing Task Team Meeting, Oct. 16-17, 1979, held at George C. Marshall Space Flight Center, Alabama, Jan. 21, 1980.

15. Design, Construction, Test and Field Support of a Containerless Payload Package for Rocket Flight, GE Final Report, NASA Contract NAS8-30797, May 20, 1977.

16. K. Kumar, and D. Das, "Magnetic Properties and Microstructures of Sprayed $SmCo_5$ Magnets Exposed to Intermediate Temperatures," J. Appl. Phys., 50(4), p. 2940, April 1979.